doi:10.1093/brain/awp257 Brain 2010: 133; 529–539 | 529

BRAIN
A JOURNAL OF NEUROLOGY

Absolute diffusivities define the landscape of white matter degeneration in Alzheimer's disease

Julio Acosta-Cabronero,[1] Guy B. Williams,[2] George Pengas[1] and Peter J. Nestor[1]

1 Herchel Smith Building for Brain and Mind Sciences, Department of Clinical Neurosciences, Neurology Unit, School of Clinical Medicine, University of Cambridge, Robinson Way, Cambridge CB2 0SZ, UK
2 Wolfson Brain Imaging Centre, Department of Clinical Neurosciences, School of Clinical Medicine, University of Cambridge, Addenbrooke's Hospital, Hills Road, Cambridge CB2 0QQ, UK

Correspondence to: Dr Julio Acosta-Cabronero,
Herchel Smith Building for Brain and Mind Sciences,
School of Clinical Medicine,
University of Cambridge,
Robinson Way,
Cambridge CB2 0SZ, UK
E-mail: jac@cantab.net

Recent imaging evidence in Alzheimer's disease suggests that neural involvement in early-stage disease is more complex than is encapsulated in the commonly held position of predominant mesial temporal lobe degeneration—there is also early posterior cingulate cortex and diencephalic damage. These findings suggest that early clinical Alzheimer's disease is underpinned by damage to an inter-connected network. If correct, this hypothesis would predict degeneration of the white matter pathways that connect this network. This prediction can be tested *in vivo* by diffusion magnetic resonance imaging. Most diffusion tensor imaging studies of white matter in neurodegenerative disorders such as Alzheimer's disease have concentrated on fractional anisotropy reductions and increased 'apparent' diffusivity; however, there is a lack of empirical biological evidence to assume that fractional anisotropy changes will necessarily capture the full extent of white matter changes in Alzheimer's disease. In this study, therefore, we undertook a comprehensive investigation of diffusion behaviour in Alzheimer's disease by analysing each of the component eigenvalues of the diffusion tensor in isolation to test the hypothesis that early Alzheimer's disease is associated with degeneration of a specific neural network. Using tract-based spatial statistics, we performed voxel-wise analyses of fractional anisotropy, axial, radial and mean diffusivities in 25 Alzheimer's disease patients compared with 13 elderly controls. We found that increased absolute (axial, radial and mean) diffusivities in Alzheimer's disease were concordant in a distribution consistent with the network hypothesis, highly statistically significant and far more sensitive than fractional anisotropy reductions. The former three measures identified confluent white matter abnormalities in parahippocampal gyrus and posterior cingulum, extending laterally into adjacent temporo-parietal regions as well as splenium and fornix. The caudal occipital lobe, temporal pole, genu and prefrontal white matter were relatively preserved. This distribution is highly consistent with expected predictions of tract degeneration from grey matter lesions identified by fluorodeoxyglucose positron emission tomography and structural magnetic resonance imaging. Concordant with results from these other imaging modalities, this pattern predominantly involves degeneration of the tracts connecting the circuit of Papez. These findings also highlight that early neuropathological processes are associated with changes of the diffusion ellipsoid that are predominantly proportional along all semi-principal axes.

Keywords: Alzheimer's disease; neurodegenerative mechanisms; diffusion tensor; white matter; tract-based spatial statistics

Abbreviations: λ_1 = axial diffusivity; DTI = diffusion tensor imaging; FA = fractional anisotropy; FDG_PET = (^{18}F)-2-fluoro-deoxy-D-glucose positron emission tomography; FDR = false discovery rate; FWE = family-wise error; MD = mean diffusivity; MRI = magnetic resonance imaging; RD = radial diffusivity; ROI = region of interest; TBSS = tract-based spatial statistics

Received May 8, 2009. Revised August 12, 2009. Accepted August 30, 2009. Advance Access publication November 13, 2009

Introduction

Structural and metabolic imaging studies in early Alzheimer's disease have highlighted several abnormalities in cortical and subcortical grey matter. Hippocampal atrophy measured by volumetric magnetic resonance imaging (MRI) is an established finding and is present in incipient (mild cognitive impairment stage) disease (Jack *et al*., 1999; Pengas *et al*., in press); comparable atrophy is also evident in the adjacent entorhinal cortex (Du *et al*., 2004). Metabolic imaging with (^{18}F)-2-fluoro-deoxy-D-glucose positron emission tomography (FDG-PET) also confirms mesial temporal lobe hypometabolism in incipient Alzheimer's disease (De Santi *et al*., 2001; Nestor *et al*., 2003), but suggests that posterior cingulate hypometabolism is the most severe metabolic lesion in early disease (Minoshima *et al*., 1997; Nestor *et al*., 2003). Although posterior cingulate hypometabolism was originally interpreted as being a remote consequence of mesial temporal lobe degeneration, recent volumetric MRI work has highlighted that this area is also atrophic in incipient Alzheimer's disease (Choo *et al*., in press; Pengas *et al*., in press). As posterior cingulate and mesial temporal lobe regions are connected via the circuit of Papez, it has been proposed that neuronal degeneration in early Alzheimer's disease may specifically involve this neuronal network (Nestor *et al*., 2003). Indeed sub-cortical elements of this circuit (mamillary bodies and anterior thalamus) are also hypometabolic in incipient disease (Nestor *et al*., 2003). The hypothesis that this is a true network degeneration would predict involvement of the white matter tracts connecting these structures (i.e. parahippocampal white matter, posterior cingulum bundle and fornix).

Mapping changes in white matter tracts is presently a major research focus for understanding development, ageing and disease of the central nervous system. The potential of diffusion MRI as a non-invasive neuroimaging tool was first highlighted when Moseley *et al*. (1990) noted hyper-intensity in diffusion-weighted acquisitions at the site of ischaemic injury. This became known as the 'light bulb' effect and has found clinical application as an early marker of stroke. A challenge in dealing with this type of acquisition is the anisotropic nature of diffusion in white matter: water molecules diffuse faster along fibre tracts than perpendicular to them due to barriers such as axonal membrane and myelin sheath—this results in an image contrast that is dependent on the spatial characteristics of the applied diffusion weighting. To characterize this dependence better, Basser *et al*. (1994) introduced the concept of diffusion tensor imaging (DTI)—(for review see Assaf and Pasternak, 2008). In this formulation, the data at each point are modelled using a second-rank tensor, visualized by a diffusion ellipsoid that represents the three-dimensional (3D) character of water molecules' diffusion. The tensor is rotationally invariant and is always aligned to the main diffusion direction at a given voxel; thus it can be decomposed into three mutually orthogonal eigenvectors and three real eigenvalues: in particular, the diffusion coefficient along the direction of maximal 'apparent' diffusion (λ_1 or axial diffusivity), and the diffusion coefficients along two orthogonal directions embedded in the plane perpendicular to the main diffusion direction (λ_2 and λ_3). The second and third eigenvalues can be averaged and expressed as so-called radial diffusivity (RD).

$$RD = \frac{(\lambda_2 + \lambda_3)}{2}$$

Further metrics can be algebraically derived to describe the relative ratio of axial to radial diffusivities, also known as anisotropy. One such metric, and the most commonly used DTI index, is fractional anisotropy or FA (Basser *et al*., 1994). In addition, the average diffusivity, known as mean diffusivity (MD) can be inferred from the overall dimensions of the diffusion ellipsoid.

$$MD = \frac{(\lambda_1 + \lambda_2 + \lambda_3)}{3}$$

DTI potentially enables mapping of white matter tract alterations in development, ageing and neurological disorders and has therefore become an important tool in the study neurodegeneration in Alzheimer's disease (Takahashi *et al*., 2002; Fellgiebel *et al*., 2004, 2008; Medina *et al*., 2006; Huang *et al*., 2007; Ringman *et al*., 2007; Zhang *et al*., 2007, 2009; Smith *et al*., in press; Damoiseaux *et al*., 2009; Mielke *et al*., 2009). The vast majority of studies to date have focused on FA changes (Chua *et al*., 2008), typically without consideration of the component eigenvalues. If changes in diffusion along the direction of the semi-major axis of the ellipsoid (λ_1) were proportional to those of the semi-minor axes (RD), however, then FA—which is a function of this ratio—would remain relatively unchanged. We hypothesized that this might be the case in early Alzheimer's disease, in which—unlike stroke where FA changes were originally noted—there may be greater changes in the absolute dimensions of the diffusion ellipsoid rather than in its shape. This prediction would translate to concordant and more sensitive results for λ_1, RD and MD when compared with FA.

In summary, the aim of this study was to use DTI measures of white matter tracts to investigate whether there was supporting evidence for the prediction that early Alzheimer's disease is associated with degeneration of structures in an inter-connected limbic–diencephalic neuronal network. Although, intuitively, FA may seem an appropriate metric to study white matter changes in neurodegenerative disease, there is neither any empirical evidence to indicate that this is the most sensitive measure nor is there evidence to suggest that other tensor behaviours could be superior in capturing the white matter tract changes in Alzheimer's disease. As such, a comprehensive analysis of diffusion measures was undertaken.

Methods

Subjects

The hypothesis was explored in a cohort of 25 patients with early-stage probable Alzheimer's disease according to Dubois criteria (Dubois *et al*., 2007) compared with 13 age- and sex-matched controls (Table 1). All controls were screened to exclude neurological or major psychiatric illness and performed normally on a global cognitive measure [the Addenbrooke's cognitive examination—revised or ACE-R (Mioshi *et al*., 2006)]. Written informed consent was obtained from all the participants and the study was approved by the local regional ethics committee.

Table 1 Demographics and cognitive features of the patients and control group

	Alzheimer's disease	Controls	*P*
Gender, M:F	15:10	5:8	NS [$\chi^2(1) = 1.59$]
Age at imaging, years	69.7 (6.3)	67.1 (5.5)	NS
Education, years	13.1 (2.6)	14.0 (2.7)	NS
MMSE at imaging/30	22.9 (4.1)	29.0 (1.2)	<0.0001
ACE-R at imaging/100	69.5 (12.5)	94.6 (3.8)	<0.0001

Values are given as mean (SD).
M = male; F = female; NS = not significant. MMSE = Mini-mental state examination; ACE-R = Addenbrooke's cognitive examination–revised

Imaging

All patients were scanned within an average of 0.9 months (SD = 1.5 months) from a cognitive assessment. MRI scans were performed on a Siemens Trio 3T system (Siemens Medical Systems, Erlangen, Germany), equipped with gradient coils capable of 45 mT/m and slew rate of 200 T/m/s. A 12 channel phased-array total imaging matrix head-coil (Siemens Medical Systems, Erlangen, Germany) was used with twice-refocused single-shot echo-planar imaging (Reese *et al*., 2003): repetition time (TR) / echo time (TE) / number of excitations (NEX) = 7800 ms/90 ms/1; matrix, 96 × 96; 63 contiguous axial slices; isotropic voxel resolution of 2 mm × 2 mm × 2 mm; bandwidth of 1628 Hz/pixel and echo spacing of 0.72 ms. The diffusion tensor was acquired with diffusion-sensitizing gradient orientations along 63 non-collinear directions ($b = 1000$ s/mm^2) that were maximally spread by considering the minimal energy arrangement of point charges on a sphere (http://www.research.att.com/~njas/electrons/dim3), and with one scan without diffusion weighting ($b = 0$ s/mm^2, $b0$). We allowed for parallel acquisition of independently reconstructed images using generalized autocalibrating partially parallel acquisitions [GRAPPA; (Griswold *et al*., 2002), acceleration factor of 2 and 39 reference lines], hence reducing the final scanning time to 8 min and 44 s.

In addition, true 3D, high-resolution, T_2-weighted images were acquired to ensure that vascular pathology was not significant in either cohort. The turbo spin echo with variable flip-angle distribution (sampling perfection with application optimized contrasts using different flip angle evolution; SPACE) pulse sequence was used with the following scan parameters: TR/TE/NEX = 3200 ms/450 ms/2; matrix, 192 × 192; 144 slices; voxel resolution, isotropic 1.25 mm × 1.25 mm × 1.25 mm. GRAPPA acceleration with a factor of 2 was also implemented, allowing a scan time of 5 min and 9 s.

T_1-weighted anatomic images were also acquired to evaluate regional differences in grey-matter density using voxel-based morphometry (Ashburner and Friston, 2000). The acquisition consisted of a 3D magnetization-prepared rapid gradient-echo pulse sequence: TR/TE/inversion time (TI)/flip angle = 2300 ms/2.86 ms/900 ms/9°, 144 slices, 192 × 192 matrix dimensions and 1.25 mm × 1.25 mm × 1.25 mm voxel size. Receiver bandwidth and echo spacing were 240 Hz/pixel and 6.7 ms, respectively; scan time was 7 min and 23 s.

The entire protocol was acquired during a single 25 min session, where the subject's brain was aligned in stereotactic space: the anterior commissure–posterior commissure line was aligned with the axial plane, and the inter-hemispheric fissure was aligned along the sagittal plane and at right angles to the coronal plane. The scanner isocentre was placed as near as possible to the centre of the thalamus in the mid-sagittal plane.

DTI analysis

The Functional MRI of the Brain (FMRIB) software library (FSL v4.0.3) (Smith *et al*., 2004) was employed to process and analyse the raw DTI data. First, each diffusion-weighted volume was affine-aligned to its corresponding $b0$ image using the FMRIB's linear image registration tool (FLIRT v5.4.2) (Jenkinson and Smith, 2001); this pre-processing step corrects for possible motion artefacts and eddy-current distortions. Prior to fitting the tensor, brain masks of each $b0$ image were generated using the brain-extraction tool (BET v2.1) (Smith, 2002) with fractional threshold, $f = 0.1$, and vertical gradient, $g = 0$. FMRIB's diffusion toolbox (FDT v2.0) was then used to fit the tensor and compute the diagonal elements (λ_1, λ_2 and λ_3), FA, RD and MD at each brain voxel.

An additional problem with DTI in degenerative diseases, however, is that atrophy can lead to systematic misregistration to template for a disease group when compared with controls, such that changes in diffusion measures [either within a region of interest (ROI) or a whole-brain voxel-based analysis] may be artefactual (Snook *et al*., 2007]. In other words, due to anatomical differences across subjects or in the presence of atrophy, a given voxel can be contaminated by greater inclusion of adjacent white matter tracts, grey matter or cerebrospinal fluid; this will, in turn, give rise to apparent changes in diffusivity that may not necessarily be due to true diffusion alterations in the tract of interest. In order to circumvent this problem, the tract-based spatial statistics (TBSS) approach (Smith *et al*., 2006) suggests a method by which the nearest most relevant tract centre in each subject's spatially normalized FA image can be projected onto a skeleton containing the centre of all major tracts 'common' to all subjects; thereby allowing voxel-wise statistics to be carried out at the tract centres only, minimizing the effect of misregistration.

As opposed to its earlier version, where every FA image was co-registered to every other one, and re-warped to the subject with the minimum mean displacement prior to affine-alignment into MNI152 standard space (Montreal Neurological Institute, McGill, USA), TBSS v1.1 provided a 1 mm isotropic FA target image (FMRIB58_FA) in standard space, to which all FA images were non-linearly warped using the image registration toolkit (Rueckert *et al*., 1999). This resulted in warped versions of each subject's FA image, which were then averaged, turned into a white matter tract skeleton and thresholded at FA > 0.2 to further limit the effects of miswarping across subjects. The skeleton was created by (i) suppressing all non-maximum FA values in each voxel's local perpendicular direction and (ii) comparing each remaining non-zero voxel with its closest neighbours, thus searching for the centre of fibre bundles. Finally, all subjects' normalized FA data were projected onto the mean FA skeleton and fed into voxel-wise statistics. Data for λ_1, RD and MD were also generated by applying the FA non-linear registration to the additional parametric maps, and projecting them onto the skeleton using identical projection vectors to those inferred from the original FA data.

TBSS uses permutation-based non-parametric inference on unsmoothed statistical maps; this method delivers better spatial localization of abnormalities than assuming normal distribution of smoothed DTI parametric maps. Non-parametric, two-sample, unpaired *t*-tests of reduced and increased DTI indices in patients compared with controls were performed using 'randomise v2.1' (included in FSL v4.1); randomise computes permutation tests on the assumption that the

null hypothesis implies complete exchangeability of the observations (Nichols and Holmes, 2002). In this study, we generated 5000 permutations of the data to test against, at threshold levels: (i) $P<0.01$ uncorrected for multiple comparisons, (ii) false discovery rate (FDR), $q<0.05$, which controls the proportion of false rejections of the null hypothesis (type I errors) among all significant voxels, and (iii) family-wise error (FWE) corrected $P<0.05$, which controls the rate of type I errors for all voxels collectively by using the null distribution of the maximal voxel-wise test statistic. FWE does not allow for control over the proportion of false positives and is usually unnecessarily conservative, particularly when data smoothing is involved; however, permutation testing offers asymptotically exact control over the false positive rate, thereby adapting easily to control the FWE rate. In addition, cluster-like structures were enhanced using a recently proposed method known as threshold-free cluster enhancement (Smith and Nichols, 2009).

Grey matter analysis

Recently, Acosta-Cabronero *et al*. (2008) found that voxel-based morphometry using the statistical parametric mapping release, SPM5 (Ashburner and Friston, 2005), can be improved by skull-stripping and bias-correcting magnetic resonance images prior to being introduced in its generative model. In this study, all scans were pre-processed using the following automated pipeline: first, skull-stripping was performed using the hybrid watershed algorithm (Ségonne *et al*., 2004) in FreeSurfer v.4.05 (http://surfer.nmr.mgh.harvard.edu), which integrates an atlas-based term constraining the shape of the brain; stripped volumes were then bias-corrected using the non-parametric non-uniform intensity normalization algorithm or N3 v.1.10 (Sled *et al*., 1998) with default arguments; and finally, a fine brain extraction that excludes venous sinuses and cerebrospinal fluid was performed using BET v.2.1 with fixed arguments: *f*, set to 0.2 and *g*, set to 0. All volumes were then spatially normalized and segmented using the unified segmentation model in SPM5. The segments were also modulated to compensate for volumetric differences introduced into the warped images. Modulation has the effect of preserving the total amount of grey matter represented by multiplying by the relative volumes. Finally, grey matter segments were smoothed using an 8 mm full width at half maximum isotropic Gaussian kernel.

A group analysis was performed to compare regional differences in grey matter density between patients and control subjects. Sex was entered into the statistical model as a nuisance co-variate. In order to maintain consistency with the permutation-based statistical approach of TBSS, the smoothed grey matter segments were assessed using the standard, permutation-based non-parametric multiple comparisons procedure: statistical non-parametric mapping. One thousand permutations of the data were generated with variance smoothing of 8 mm full width at half maximum, masked by the relative threshold of 0.2 and statistical threshold of $q<0.05$ (FDR).

Results

TBSS results for increased FA and reduced diffusivities in 25 mild Alzheimer's disease patients compared with 13 elderly controls did not show any statistically significant difference at $P<0.01$ uncorrected for multiple comparisons. The reduced FA contrast (Fig. 1), however, identified small discrete areas of significant change in the white matter of the right temporal lobe, right posterior cingulate region and right parieto-occipital region. FA reductions were also identified in the fornix (see Fig. 1: sagittal slice $x=0$ mm; coronal slice $y=-4$ mm; axial slice $z=10$ mm) as well as two small areas in the right cerebellar hemisphere and ponto-medullary junction. Results of the analyses are shown at uncorrected $P<0.01$ overlaid onto the MNI152 template and the mean FA skeleton. The results for increased λ_1, RD and MD (Fig. 1) were broadly concordant with each other and far more extensive than for FA. Axial and mean diffusivity clusters of significance were slightly more extensive than those for RD. Axial, radial and mean diffusivity contrasts identified similar significant changes to those seen with FA in fornix and cerebral white matter, but not in the brainstem or cerebellum. Unlike FA, however, changes in λ_1, RD and MD were bilateral and confluent involving the white matter of caudal cingulum bundle, parahippocampal gyrus and spreading into adjacent lateral white matter areas of the caudal temporal and parietal regions. The caudal corpus callosum was also abnormal with all three measures, whereas there was relative sparing of caudal occipital lobe, temporal pole, prefrontal white matter and rostral corpus callosum. The rendered volumes and overlays shown in Fig. 2, using axial diffusivity, illustrate in detail this distribution of white matter abnormalities.

At a FDR of 0.05, the λ_1, RD and MD FDR-corrected *P* thresholds (0.0088, 0.0082 and 0.0094, respectively) were almost equivalent to the *ad hoc* uncorrected significance level proposed above (Fig. 3A). The more conservative FWE rate of 0.05 (Fig. 3B) led to an expected decrease in sensitivity, but overall produced very similar clusters of significance to those for uncorrected and FDR-corrected critical values. In contrast, all FA suprathreshold voxels were expected to be false positives at these multiple comparison correction thresholds. Repeating the analyses after independently controlling for gender, age and education level difference yielded identical results.

The distribution of grey matter abnormalities in this cohort from the voxel-based morphometry analysis was in agreement with the above TBSS result (Fig. 4). Loss of grey matter density in the Alzheimer's disease group was most significant in the hippocampus, followed by entorhinal region. This extended to a less significant extent into temporal neocortex and insula. The posterior cingulate cortex was also significantly atrophic.

Discussion

The λ_1, RD and MD findings using the TBSS method offer what we propose is the most comprehensive view of the landscape of white matter tract degeneration in early Alzheimer's disease to date; and offers strong evidence that early Alzheimer's disease is associated with specific degeneration of a limbic–diencephalic neuronal network. Mesial temporal lobe atrophy and posterior temporo-parietal association cortex hypometabolism are established features of Alzheimer's disease (Nestor *et al*., 2004). Studies in recent years have identified focal posterior cingulate hypometabolism as the earliest physiological lesion (Minoshima *et al*., 1997); this area was subsequently found to be as significantly atrophic as the hippocampus in very early Alzheimer's

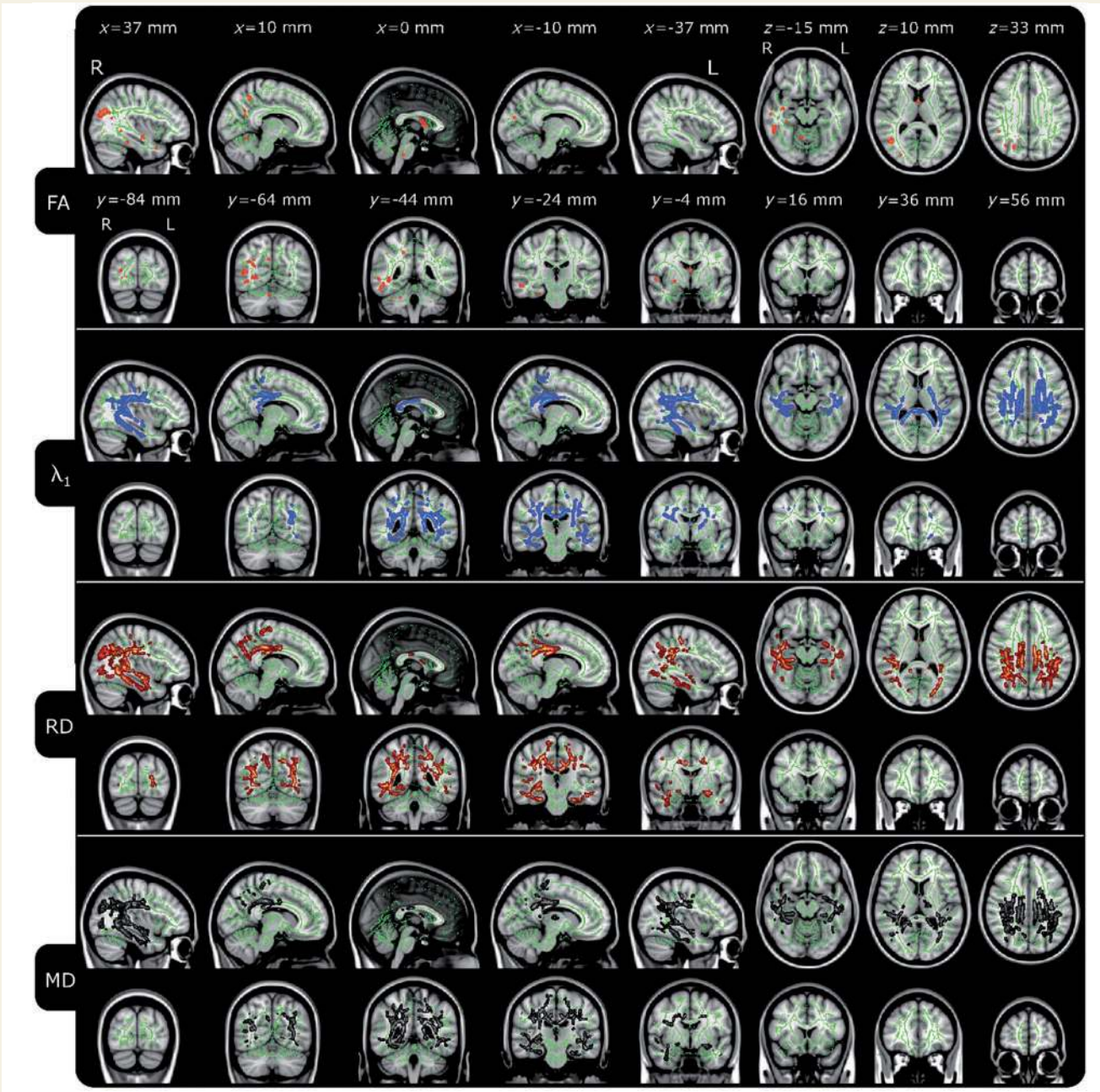

Figure 1 TBSS results for reduced FA and increased absolute diffusivities in Alzheimer's disease patients. Thresholded (uncorrected $P<0.01$) statistical maps for reduced FA and increased λ_1, RD and MD in 25 early-stage Alzheimer's disease patients compared with 13 elderly controls. TBSS results show largely confluent and concordant results for all diffusivity measures in temporo-parietal white matter, posterior cingulum, splenium and fornix; FA, in contrast, was far less sensitive.

disease (Pengas *et al*., in press). Evidence of lesions in mesial temporal and posterior cingulate regions was extended by the observation that hypometabolism in these regions as well as diencephalic structures (anterior thalamus and mamillary body) was specifically associated with very early stage Alzheimer's disease (Nestor *et al*., 2003). This led to the conjecture that these areas were degenerating as part of a functionally and anatomically integrated system (Nestor *et al*., 2003, 2006). These various observations would predict that the landscape of axonal tract degeneration in early Alzheimer's disease would include white matter of the parahippocampal gyrus extending to, and continuing along, the posterior cingulum bundle; that there would be extension of white matter degeneration from these areas into lateral (especially) posterior temporo-parietal areas; that preferential degeneration of these posterior associations cortices would lead to preferential degeneration of inter-hemispheric white matter connections passing through the caudal, as opposed to rostral, corpus callosum; that fibres

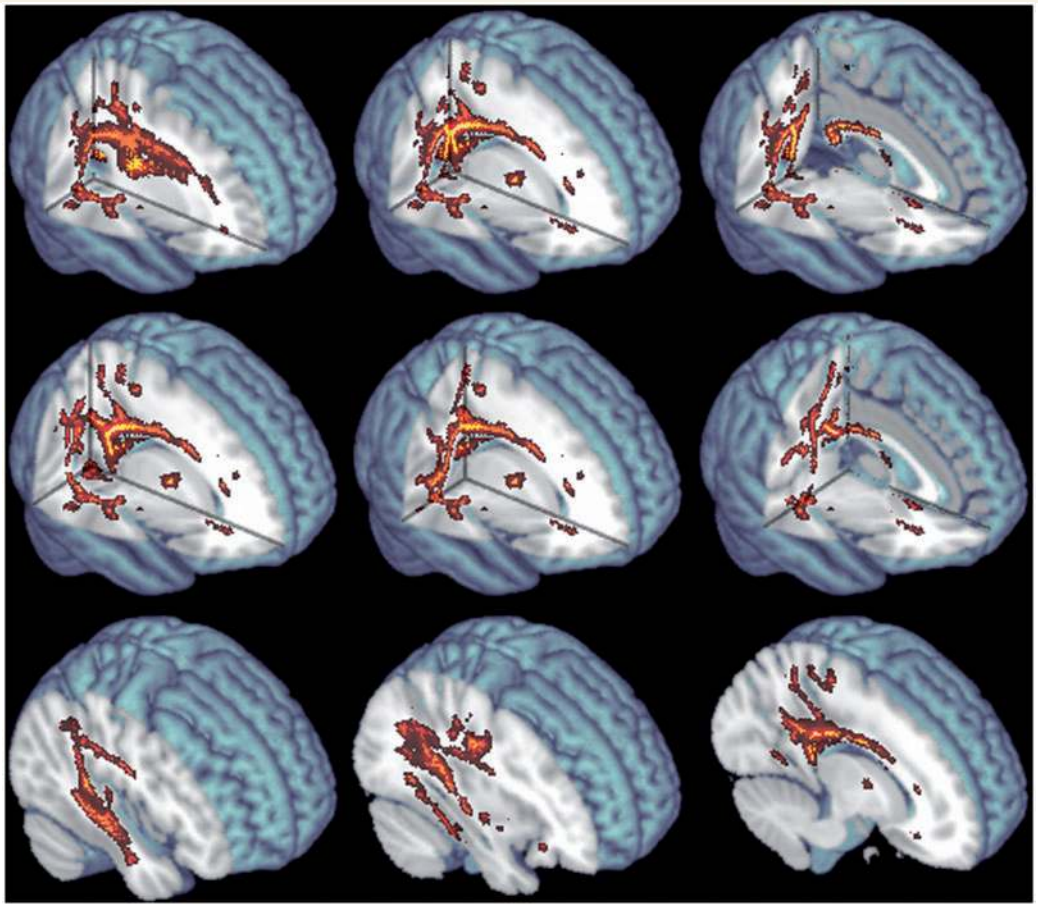

Figure 2 TBSS results for increased λ_1 (uncorrected $P<0.01$) in 25 early-stage Alzheimer's disease patients compared with 13 elderly controls. Note the contiguous involvement of the parahippocampal and posterior cingulum white matter as well as the fornix (top right panel).

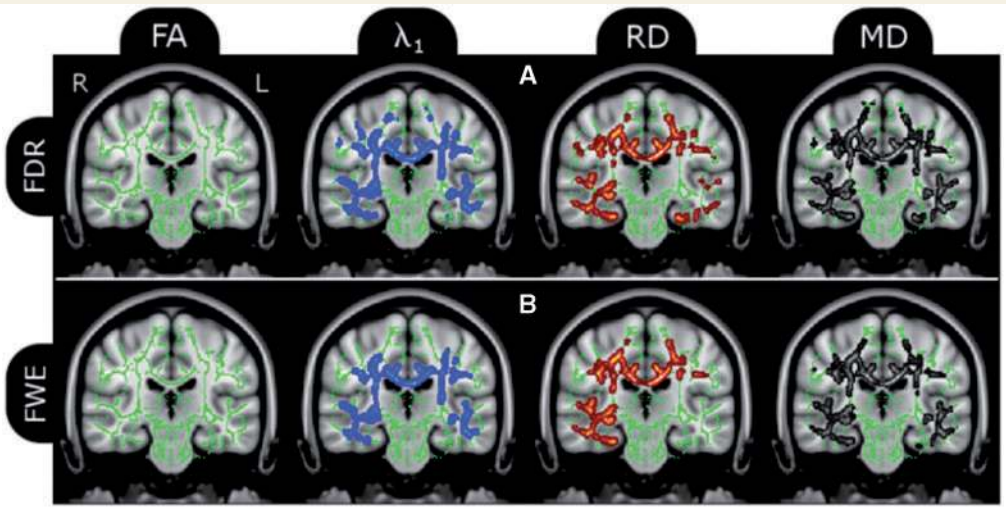

Figure 3 TBSS results with correction for multiple comparisons. Statistical maps for reduced FA and increased λ_1, RD and MD in 25 mild Alzheimer's disease patients compared with 13 controls thresholded at (**A**) FDR, $q<0.05$ and (**B**) FWE-corrected $P<0.05$. FA differences were not significant when corrected for multiple testing, whereas results for diffusivity measures were concordant and highly significant.

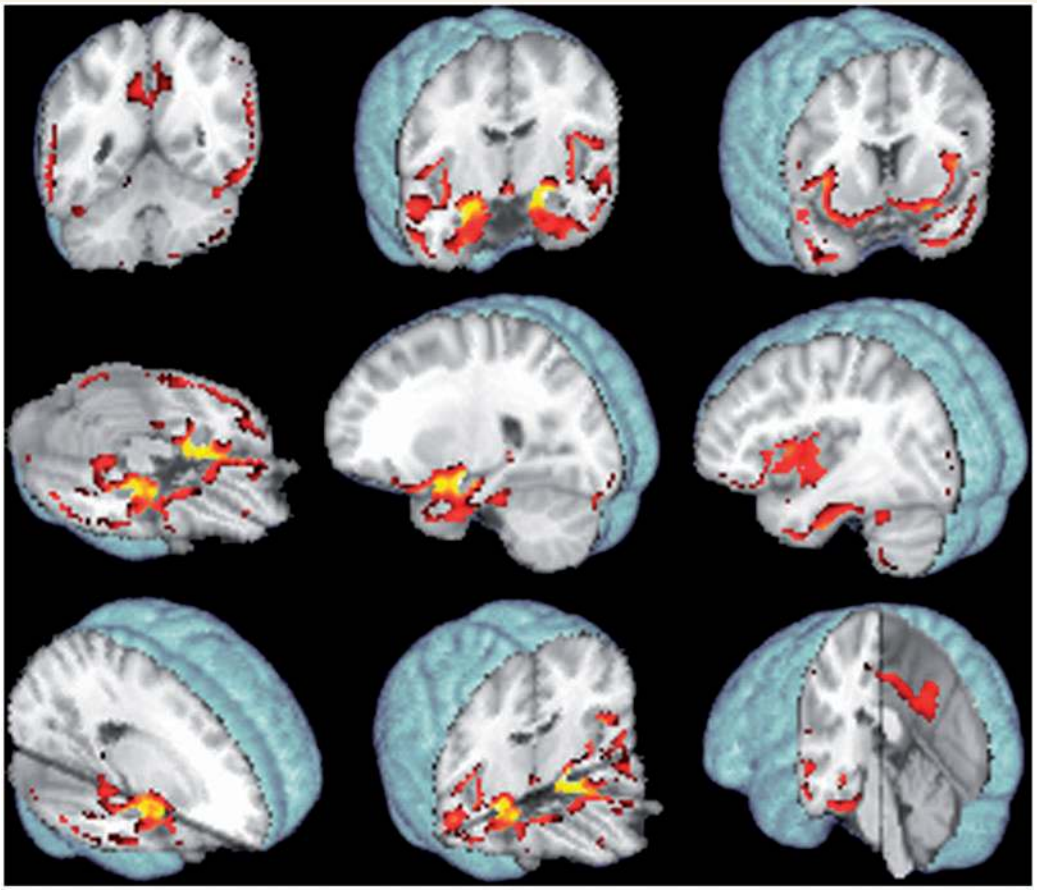

Figure 4 Non-parametric statistical result of regional grey matter density loss in 25 mild Alzheimer's disease patients compared with 13 healthy controls at $q < 0.05$ (FDR).

connecting mesial temporal lobe and diencephalon via the fornix would degenerate; and that there would be relative preservation of white matter in prefrontal, temporal pole and caudal occipital areas. The findings for λ_1, RD and MD, although not to such an extent for FA, identified precisely this distribution of white matter changes.

Consistent with this network hypothesis that links cortical degeneration and white matter pathways, the voxel-based morphometry results from the present cohort confirmed that the patient group had atrophy of the temporal lobes (especially hippocampus), and, to a lesser degree, the posterior cingulate cortex. Greater hippocampal involvement might suggest that this region is the primary driver of network degeneration—an interpretation consistent with early neurofibrillary tangle deposition in the mesial temporal lobe (Braak and Braak, 1991). It should be noted, however, that voxel-based morphometry may lack sensitivity in the posterior cingulate region; for instance, recently two independent manual volumetric studies of very early Alzheimer's disease (scanned at the mild cognitive impairment stage) both found significant posterior cingulate atrophy (Choo *et al*., in press; Pengas *et al*., in press) that was at least as severe as that of the hippocampus; pre-symptomatic Alzheimer's disease patients (autosomal dominant mutation carriers) have accelerated rates of atrophy using the serial fluid co-registration technique in both posterior cingulate and hippocampus but in no other regions (Scahill *et al*., 2002); and, finally, cortical thickness measurements in Alzheimer's disease suggest focal thinning of the posterior cingulate/precuneus region compared with the remainder of the mesial (inter-hemispheric) cortical surface (Du *et al*., 2007).

A recent study highlighted a remarkable homology between the atrophy profile in Alzheimer's disease (mesial temporal-posterior cingulate/precuneus-lateral temporo-parietal cortex) and an intrinsic functional connectivity network in healthy volunteers derived from resting state functional (f)MRI (Seeley *et al*., 2009). The present DTI findings provide very strong support for a direct relationship between these two observations, in that the anatomical connections between these structures were precisely those that were preferentially involved in the current study.

The current results are also of interest to contrast with the default mode network hypothesis in Alzheimer's disease. It has been noted that there is a striking homology between regions of high resting state fMRI activity in healthy volunteers (default mode) and the distribution of amyloid (using Pittsburgh Compound-B-PET) in Alzheimer's disease patients: in each the highlighted regions are posterior cingulate/precuneus/lateral temporo-parietal cortex and ventral frontal cortex (Buckner *et al*., 2005). Synaptic dysfunction in Alzheimer's disease, as

measured with FDG-PET, is only partially consistent with this distribution, in that the posterior components are abnormal early whereas the frontal component is not a prominent early feature. As already discussed, the present DTI results sided with FDG-PET in demonstrating preferential degeneration of the limbic–diencephalic network—the nodes of which had been shown previously to be specifically hypometabolic in very early Alzheimer's disease (Nestor *et al*., 2003); the present results did not, however, identify significant ventral prefrontal white matter changes. Bringing these streams together suggests that there is not simply a stepwise progression from local resting state activity in health, to local amyloid deposition and to local neuronal degeneration. Assuming (i) that default mode activity and amyloid distribution are not simply coincidental and (ii) that their overlap is an important early trigger to a cascade of events that causes dementia in Alzheimer's disease, one then has to reconcile why the neural network that degenerates first in Alzheimer's disease is only partially overlapping. One possibility could be that although amyloid deposits in both places, there are additional factors that make the posterior regions selectively vulnerable to neurodegeneration and that this, in turn, involves the whole limbic–diencephalic network. If this speculation were correct then identifying those additional factors would be of considerable importance. The anatomical relationship of posterior cingulate to mesial temporal lobe suggests that one potential candidate is that this is the pathway by which, as Price and Morris (1999) speculated, the presence of amyloid turns a ubiquitous and relatively benign age-associated tauopathy towards an accelerated phase of neurofibrillary tangle formation and neuronal loss.

Turning to the methodological aspects of this study, although DTI is an established method to visualize diffusional properties of white matter, the biological underpinning of tensor changes remains incompletely understood. Using FA changes as a marker of axonal integrity imposes the assumption that degeneration will give rise to changes in the shape of the diffusion ellipsoid (Fig. 5A and B). It is widely believed, for instance, that phenomena such as demyelination and axonal loss may cause a scenario in which FA reductions are driven by enhanced radial diffusion and constant axial diffusivity coefficient (Fig. 5A) (Beaulieu, 2002; Song *et al*., 2002). In contrast, simultaneous axial diffusivity reduction and radial diffusivity increase is thought to be associated to fibre re-organization (Fig. 5B) (Dubois *et al*., 2008). It is conceivable, however, that contributions of other neurobiological processes involved in white matter tract degeneration such as destruction of neurofibrils and glial alterations can give rise to tensor behaviours that are not fully captured by anisotropy changes. FA may lack sensitivity if water diffusion changes proportionally along the direction of all three eigenvectors (Fig. 5C). Furthermore, it does neither follow that these biological processes will be the same across different pathologies nor even within a single pathology at different stages of illness: differential effects on glia, mechanisms of axonal degeneration, inflammatory responses and even the rate of degeneration could give rise to different

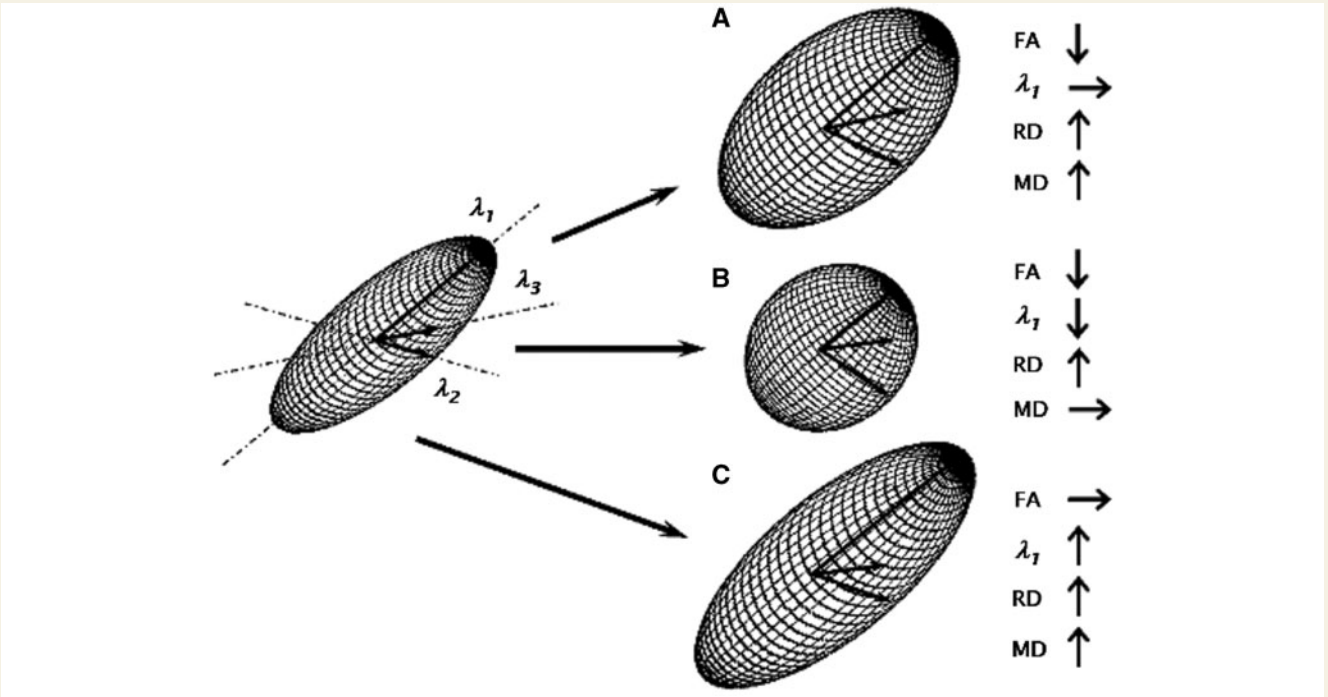

Figure 5 Possible scenarios of change to the diffusion ellipsoid in neurodegeneration. (**A**) Description of the behaviour of the ellipsoid if constriction and tortuosity is reduced only on the plane perpendicular to the main diffusion direction. Thus, radial diffusivity ($RD = (\lambda_2 + \lambda_3)/2$) increases while axial diffusivity (λ_1) remains constant, leading to FA reduction and overall increase of apparent diffusion (MD). (**B**) Representation of a hypothetical ellipsoid product of water molecules diffusing slower axially (λ_1 reduction) and faster transversely (RD increase), leaving MD constant but reducing FA. (**C**) Illustration of a scenario where less restricted media allows water molecules to diffuse faster in all directions. FA remains constant due to the simultaneous increase in λ_1, λ_2 and λ_3.

tensor behaviours in different pathological states. In summary, exploration of the full tensor behaviour would be advantageous in studying all degenerative diseases rather than assuming that a single metric (such as FA) is sufficiently sensitive to different pathological states.

In order to explore comprehensively the behaviour of the diffusion tensor in neurodegeneration, we performed TBSS analyses, not only of FA maps, but also of axial, radial and total mean diffusities (λ_1, RD and MD, respectively) in Alzheimer's disease patients compared with elderly controls. The concordance of observations for the absolute diffusivity measures and the gross lack of sensitivity of FA, caused by smaller group mean differences in the latter, are consistent with the hypothesis that early neurodegeneration in Alzheimer's disease is associated with predominantly proportional tensor variations in all three dimensions (Fig. 5C). This conclusion was underlined by the observation that changes in λ_1, RD and MD, but not FA, survived correction for multiple comparisons using either FDR or, the most stringent, FWE methods. These findings suggest that FA is not the appropriate metric for studying white matter tract degeneration in Alzheimer's disease, a finding that could prove true of other neurodegenerative diseases though this would need to be demonstrated in these different diseases rather than assuming that it is the case.

It is usually assumed that the main diffusion direction is aligned to white matter tracts, and that radial diffusivities, which average diffusion perpendicular to fibre bundles, are modulated by the extracellular distance between membranes, axon diameter and degree of myelination. Consequently, it is thought that loss of fibre tracts and disruption of myelin sheath during neurodegeneration should not affect longitudinal diffusivities, and could uniquely be explained by enhanced transverse diffusion and therefore, apparent FA reductions (Beaulieu, 2002; Song *et al*., 2002). This simplistic approach, however, does not include the effect of other plausible biophysical phenomena in neurodegenerative disorders such as fibre re-organization, increase in membrane permeability, destruction of intracellular compartments and glial alterations (Beaulieu, 2002). The magnitude of the impact of these processes on the diffusion tensor is unknown, but it is plausible that they may induce water molecules to diffuse faster in unanticipated directions. This may be the case in this study, where we observed regions of significant increase of λ_1 that were concordant to those of RD and MD, resulting in insubstantial anisotropy changes. These results highlight the importance of exploring the full power of the diffusion tensor, and indicate that changes in the size of the diffusion ellipsoid (i.e. changes in diffusion eigenvalues that may be the product of complex interactions between several neurodegenerative processes) are more sensitive and more biologically plausible than changes in the anisotropy of the ellipsoid.

It was clear, however, that λ_1 increase was slightly more emphatic than the change in transverse diffusion (Fig. 3); this should lead to a slight change in FA, even though FA is inherently less sensitive because RD and λ_1 changed in the same direction. Nevertheless, the slightly disproportionate effect on λ_1 might be the reason why significant changes in FA have been reported in previous ROI studies of Alzheimer's disease (e.g. Mielke *et al*., 2009; Zhang *et al*., 2009). In other words, subtle changes in FA can be detected within ROIs that do not survive more stringent whole-brain statistical analysis. Notably, however, one ROI study that looked at FA and MD found that the latter measure was more sensitive within ROIs (Fellgiebel *et al*., 2004), consistent with the present results. Another important consideration, and the reason that ROI analyses were avoided in the present study, is that it also possible that previously reported FA changes from ROI analyses may be, to a significant degree, artefactual. Even a subtle amount of atrophy in a tract of interest could lead to a systematic mis-sampling of that tract between patient and control groups. For instance, when an ROI is applied, subtle distortion of the anatomy (secondary to atrophy) means that the ROI in the disease group could include a greater amount of an adjacent tract which would, in turn, translate to a significant FA difference that was not actually a consequence of degeneration in the tract of interest (i.e. control's ROI = tract *X*; patient's ROI = tract *X* + *Y*). Colour-coding of tracts prior to ROI placement has been proposed to minimize this problem (Fellgiebel *et al*., 2005); however, because this colour coding only highlights the three principal orthogonal planes, it is unlikely that such an approach can completely eliminate the effect of contamination from adjacent tracts which might run in any direction rather than only being orthogonal to a tract of interest.

In summary, using TBSS to minimize preprocessing and analytic inaccuracies, this study investigated changes in both the anisotropic properties of diffusion (FA) and non-fractional measures of diffusivity (λ_1, RD and MD). The results indicated that the latter are more sensitive than FA in Alzheimer's disease, seriously challenging the notion that changes in axonal integrity can be simply captured by FA reductions. It is still premature to conclude that DTI can fully describe the physical phenomena that characterize white matter degeneration in Alzheimer's disease, but the results are very encouraging in that the diffusion tensor is highly sensitive to changes in mild Alzheimer's disease patients, and that these changes are highly concordant with predictions of expected white matter change derived from prior knowledge of other imaging modalities. Beyond Alzheimer's disease, these measures may equally inform the nature of neural network changes in other neurodegenerative diseases and are also of potential relevance to normal maturation and ageing. With respect to Alzheimer's disease, the findings offer compelling evidence that the limbic–diencephalic network is selectively vulnerable to the degenerative process. Understanding what makes the neurons in this network preferentially degenerate is a key question for future research. Identification of molecular differences in this neuronal network compared with others less susceptible to degeneration in Alzheimer's disease might offer a bridgehead to a deeper mechanistic understanding of the pathogenesis of this disease.

Acknowledgements

We are also grateful for support from the National Institute for Health Research (Cambridge Biomedical Research Centre).

Funding

Medical Research Council, UK (to P.J.N.); Alzheimer's Research Trust (to G.P.).

References

Acosta-Cabronero J, Williams GB, Pereira JMS, Pengas G, Nestor PJ. The impact of skull-stripping and radio-frequency bias correction on grey-matter segmentation for voxel-based morphometry. NeuroImage 2008; 39: 1654–65.

Ashburner J, Friston KJ. Voxel-based morphometry—the methods. Neuroimage 2000; 11: 805–21.

Ashburner J, Friston KJ. Unified segmentation. Neuroimage 2005; 26: 839–51.

Assaf Y, Pasternak O. Diffusion tensor imaging (DTI)-based white matter mapping in brain research: a review. J Mol Neurosci 2008; 34: 51–61.

Basser PJ, Mattiello J, LeBihan D. MR diffusion tensor spectroscopy and imaging. Biophys J 1994; 66: 259–67.

Beaulieu C. The basis of anisotropic water diffusion in the nervous system—a technical review. NMR Biomed 2002; 15: 435–55.

Braak H, Braak E. Demonstration of amyloid deposits and neurofibrillary changes in whole brain sections. Brain Pathol 1991; 1: 213–6.

Buckner RL, Snyder AZ, Shannon BJ, LaRossa G, Sachs R, Fotenos AF, et al. Molecular, structural, and functional characterization of Alzheimer's disease: evidence for a relationship between default activity, amyloid, and memory. J Neurosci 2005; 25: 7709–17.

Choo IH, Lee DY, Oh JS, Lee JS, Lee DS, Song IC, et al. Posterior cingulate cortex atrophy and regional cingulum disruption in mild cognitive impairment and Alzheimer's disease. Neurobiol Aging 2009; in press doi:10.1016/j.neurobiolaging.2008.06.015).

Chua TC, Wen W, Slavin MJ, Sachdev PS. Diffusion tensor imaging in mild cognitive impairment and Alzheimer's disease: a review. Curr Opin Neurol 2008; 21: 83–92.

Damoiseaux JS, Smith SM, Witter MP, Sanz-Arigita EJ, Barkhof F, Scheltens P, et al. White matter tract integrity in aging and Alzheimer's disease. Hum Brain Mapp 2009; 30: 1051–9.

De Santi S, de Leon MJ, Rusinek H, Convit A, Tarshish CY, Roche A, et al. Hippocampal formation glucose metabolism and volume losses in MCI and Alzheimer's disease. Neurobiol Aging 2001; 22: 529–39.

Du AT, Schuff N, Kramer JH, Ganzer S, Zhu XP, Jagust WJ, et al. Higher atrophy rate of entorhinal cortex than hippocampus in Alzheimer's disease. Neurology 2004; 62: 422–7.

Du AT, Schuff N, Kramer JH, Rosen HJ, Gorno-Tempini ML, Rankin K, et al. Different regional patterns of cortical thinning in Alzheimer's disease and frontotemporal dementia. Brain 2007; 130: 1159–66.

Dubois B, Feldman HH, Jacova C, Dekosky ST, Barberger-Gateau P, Cummings J, et al. Research criteria for the diagnosis of Alzheimer's disease: revising the NINCDS-ADRDA criteria. Lancet Neurol 2007; 6: 734–46.

Dubois J, Dehaene-Lambertz G, Perrin M, Mangin JF, Cointepas Y, Duchesnay E, *et al*. Asynchrony of the early maturation of white matter bundles in healthy infants: quantitative landmarks revealed noninvasively by diffusion tensor imaging. Hum Brain Mapp 2008; 29: 14–27.

Fellgiebel A, Muller MJ, Wille P, Dellani PR, Scheurich A, Schmidt LG, et al. Color-coded diffusion-tensor-imaging of posterior cingulate fiber tracts in mild cognitive impairment. Neurobiol Aging 2005; 26: 1193–8.

Fellgiebel A, Schermuly I, Gerhard A, Keller I, Albrecht J, Weibrich C, et al. Functional relevant loss of long association fibre tracts integrity in early Alzheimer's disease. Neuropsychologia 2008; 46: 1698–706.

Fellgiebel A, Wille P, Muller MJ, Winterer G, Scheurich A, Vucurevic G, et al. Ultrastructural hippocampal and white matter alterations in mild cognitive impairment: a diffusion tensor imaging study. Dement Geriatr Cogn Disord 2004; 18: 101–8.

Griswold MA, Jakob PM, Heidemann RM, Nittka M, Jellus V, Wang J, et al. Generalized autocalibrating partially parallel acquisitions (GRAPPA). Magn Reson Med 2002; 47: 1202–10.

Huang J, Friedland RP, Auchus AP. Diffusion tensor imaging of normal-appearing white matter in mild cognitive impairment and early Alzheimer disease: preliminary evidence of axonal degeneration in the temporal lobe. AJNR Am J Neuroradiol 2007; 28: 1943–8.

Jack CR Jr, Petersen RC, Xu YC, O'Brien PC, Smith GE, Ivnik RJ, et al. Prediction of Alzheimer's disease with MRI-based hippocampal volume in mild cognitive impairment. Neurology 1999; 52: 1397–403.

Jenkinson M, Smith S. A global optimisation method for robust affine registration of brain images. Med Image Anal 2001; 5: 143–56.

Medina D, DeToledo-Morrell L, Urresta F, Gabrieli JD, Moseley M, Fleischman D, et al. White matter changes in mild cognitive impairment and Alzheimer's disease: a diffusion tensor imaging study. Neurobiol Aging 2006; 27: 663–72.

Mielke MM, Kozauer NA, Chan KC, George M, Toroney J, Zerrate M, et al. Regionally-specific diffusion tensor imaging in mild cognitive impairment and Alzheimer's disease. Neuroimage 2009; 46: 47–55.

Minoshima S, Giordani B, Berent S, Frey KA, Foster NL, Kuhl DE. Metabolic reduction in the posterior cingulate cortex in very early Alzheimer's disease. Ann Neurol 1997; 42: 85–94.

Mioshi E, Dawson K, Mitchell J, Arnold R, Hodges JR. The Addenbrooke's cognitive examination revised (ACE-R): a brief cognitive test battery for dementia screening. Int J Geriatr Psychiatry 2006; 21: 1078–85.

Moseley ME, Kucharczyk J, Mintorovitch J, Cohen Y, Kurhanewicz J, Derugin N, et al. Diffusion-weighted MR imaging of acute stroke: correlation with T2-weighted and magnetic susceptibility-enhanced MR imaging in cats. AJNR Am J Neuroradiol 1990; 11: 423–9.

Nestor PJ, Fryer TD, Hodges JR. Declarative memory impairments in Alzheimer's disease and semantic dementia. Neuroimage 2006; 30: 1010–20.

Nestor PJ, Fryer TD, Smielewski P, Hodges JR. Limbic hypometabolism in Alzheimer's disease and mild cognitive impairment. Ann Neurol 2003; 54: 343–51.

Nestor PJ, Scheltens P, Hodges JR. Advances in the early detection of Alzheimer's disease. Nat Med 2004; 10 (Suppl): S34–41.

Nichols TE, Holmes AP. Nonparametric permutation tests for functional neuroimaging: a primer with examples. Hum Brain Mapp 2002; 15: 1–25.

Pengas G, Hodges JR, Watson P, Nestor PJ. Focal posterior cingulate atrophy in incipient Alzheimer's disease. Neurobiol Aging in press; (doi:10.1016/j.neurobiolaging.2008.03.014).

Price JL, Morris JC. Tangles and plaques in nondemented aging and ''preclinical'' Alzheimer's disease. Ann Neurol 1999; 45: 358–68.

Reese TG, Heid O, Weisskoff RM, Wedeen VJ. Reduction of eddy-current-induced distortion in diffusion MRI using a twice-refocused spin echo. Magn Reson Med 2003; 49: 177–82.

Ringman JM, O'Neill J, Geschwind D, Medina L, Apostolova LG, Rodriguez Y, et al. Diffusion tensor imaging in preclinical and presymptomatic carriers of familial Alzheimer's disease mutations. Brain 2007; 130: 1767–76.

Rueckert D, Sonoda LI, Hayes C, Hill DLG, Leach MO, Hawkes DJ. Non-rigid registration using free-form deformations: application to breast MR images. IEEE Trans Med Imaging 1999; 18: 712–21.

Scahill RI, Schott JM, Stevens JM, Rossor MN, Fox NC. Mapping the evolution of regional atrophy in Alzheimer's disease: unbiased analysis of fluid-registered serial MRI. Proc Natl Acad Sci USA 2002; 99: 4703–7.

Seeley WW, Crawford RK, Zhou J, Miller BL, Greicius MD. Neurodegenerative diseases target large-scale human brain networks. Neuron 2009; 62: 42–52.

Ségonne F, Dale AM, Busa E, Glessner M, Salat D, Hahn HK, et al. A hybrid approach to the skull stripping problem in MRI. Neuroimage 2004; 22: 1060–75.

Sled JG, Zijdenbos AP, Evans AC. A nonparametric method for automatic correction of intensity nonuniformity in MRI data. IEEE Trans Med Imaging 1998; 17: 87–97.

Smith CD, Chebrolu H, Andersen AH, Powell DA, Lovell MA, Xiong S, et al. White matter diffusion alterations in normal women at risk of Alzheimer's disease. Neurobiol Aging in press [doi:10.1016/j.neurobiolaging.2008.08.006].

Smith SM. Fast robust automated brain extraction. Hum Brain Mapp 2002; 17: 143–55.

Smith SM, Jenkinson M, Johansen-Berg H, Rueckert D, Nichols TE, Mackay CE, et al. Tract-based spatial statistics: voxelwise analysis of multi-subject diffusion data. Neuroimage 2006; 31: 1487–505.

Smith SM, Jenkinson M, Woolrich MW, Beckmann CF, Behrens TE, Johansen-Berg H, et al. Advances in functional and structural MR image analysis and implementation as FSL. Neuroimage 2004; 23 (Suppl 1): S208–19.

Smith SM, Nichols TE. Threshold-free cluster enhancement: addressing problems of smoothing, threshold dependence and localisation in cluster inference. Neuroimage 2009; 44: 83–98.

Snook L, Plewes C, Beaulieu C. Voxel based versus region of interest analysis in diffusion tensor imaging of neurodevelopment. Neuroimage 2007; 34: 243–52.

Song SK, Sun SW, Ramsbottom MJ, Chang C, Russell J, Cross AH. Dysmyelination revealed through MRI as increased radial (but unchanged axial) diffusion of water. Neuroimage 2002; 17: 1429–36.

Takahashi S, Yonezawa H, Takahashi J, Kudo M, Inoue T, Tohgi H. Selective reduction of diffusion anisotropy in white matter of Alzheimer disease brains measured by 3.0 Tesla magnetic resonance imaging. Neurosci Lett 2002; 332: 45–8.

Zhang Y, Schuff N, Du AT, Rosen HJ, Kramer JH, Gorno-Tempini ML, et al. White matter damage in frontotemporal dementia and Alzheimer's disease measured by diffusion MRI. Brain 2009; 132: 2579–92.

Zhang Y, Schuff N, Jahng GH, Bayne W, Mori S, Schad L, et al. Diffusion tensor imaging of cingulum fibers in mild cognitive impairment and Alzheimer disease. Neurology 2007; 68: 13–9.